

# Study on Reducing Cogging Torque of Interior PM Motor for Agricultural Electric Vehicle

Ju-Hee Cho\*, Yong-Un Park\*\* and Dae-Kyong Kim\*\*\*

**Abstract** –This paper proposes a new design of rotor shape of Interior Permanent Magnet Synchronous Motor (IPMSM) used for agricultural electric vehicle (AEV). The distribution of the residual magnetic flux density at the air gap is modified by rotor surface shape and V-type magnet angle. As a result, cogging torque and physical characteristic have been improved, and back electromotive force (back-EMF) of the suggested model has been improved to be closest to sine wave form compared to initial model. The validity of the proposed rotor shape optimization is confirmed by the manufactured IPM rotor core and measured the performance of the cogging torque.

**Keywords:** AEV, cogging torque, IPMSM

## 1. Introduction

Agriculture contributes 9% to the global warming problems according to a report by the Intergovernmental Panel on Climate Change (IPCC). It was found the agriculture accounts for about 3% of total emitted carbon dioxide in world. In order to reduce the emission of carbon dioxide from agricultural vehicles and to help protect the global the global climate, it is essential that agricultural electric vehicle (AEV) is developed [1]. Accordingly, many countries, especially the advanced countries, show the trend of moving to electric operating system even for agricultural use. Even in the midst of active research and development in electric operating system for such high-demand products as automobiles, we find a conspicuous lack of research and development of agricultural electric vehicles. At the same time, given the steady increase of oil price in the international market and the possibility of technological monopoly by a few advanced countries, it is imperative to put our effort in the development of high-efficiency operating motors, the core of operating system for the electric vehicles [2].

Due to the nature of agricultural farm machinery Electric vehicles driving in the natural space, so the smooth operation in harsh environmental conditions, so be capable

of driving motors must satisfy both the durability and reliability and are installed in confined spaces, high efficiency and small size and light weight are essential demand. To meet these requirements permanent magnet synchronous motor is mainly used. Depending on the structure of the rotor permanent magnet synchronous motors Surface Permanent Magnet (SPM) and Interior Permanent Magnet (IPM) IPM motor which can be divided into high-speed operation utilizing reluctance torque can be easily and have the advantage of driving is a trend that is being widely applied to the motor.

Especially, interior permanent-magnet synchronous motors (IPMSMs) with potential high efficiency, high power factor, high power density and excellent flux weakening capability is one of the best choices for the electric vehicle (EV) propulsion system [2]. However, the IPM motor has a feature of large cogging torque by the difference caused by unbalanced magnetic reluctance because of the shape of stator and rotor. As cogging torque could cause the vibration and noise of the motor, it is essential to design to reduce the cogging torque [3]-[6].

In this paper, a new rotor shape design of IPM motor for reducing cogging torque is suggested where the distribution of the residual magnetic flux density at the air gap is modified by rotor surface shape and V-type magnet angle. The finite-element analysis (FEA) is applied for the optimal shape design of rotor surface shape and V-type magnet angle, because the IPM motor has an extreme saturation in rotor core. This paper shows the validity of the proposed rotor shape optimization, the manufactured IPM rotor core and the performance of the cogging torque.

\* Korea Electronics Technology Institute. (jhcho@keti.re.kr)

\*\* Dept. of Electrical Engineering, Suncheon National University, Korea. (pyu77@suncheon.ac.kr)

\*\*\* Dept. of Electrical Control Engineering, Suncheon National University, Korea. (dkkim@suncheon.ac.kr)

## 2. Design Model

Suggested motor of this paper is 10kW class of 8pole12slot structure IPMSM for Electric Drive Tractor. It shows IPMSM design spec suggested by Table 1.

**Table 1.** Design Specification of the IPMSM

Parameter	Unit	Value
Cont.Power	kW	10
Cont.Torque	Nm	31.8
Cont.Speed	rpm	3000
Input Voltage	VDC	378~252
Max.Power	kW	17
Max.Efficiency	%	93

## 3. Initial Model Design of Drive Motor for Electric Drive Tractor

### 3.1 Set Number of Slot & Pole

Combination of number of slot & pole of drive motor must be chosen by serving a performance objectives condition and considering right matching. To minimize cogging torque, number of slot & pole combination of 3-phase drive motor should be decided.

Number of slot is considered for process and cost. Number of pole is considered for shape of rotor, material of permanent magnet, and rotation speed of motor, so 8 pole 12 slot is chosen. To shorten diameter of coil, it consists of 4 parallel circuits.

### 3.2 Set Determine the initial dimensions

The initial dimension of the driving motors can be inferred from torque equation of motor of equation (1)

$$T = KD_r^2 L_r \tag{1}$$

In this case, K: static output, D<sub>r</sub>: rotor diameter, L<sub>r</sub>: lamination stack. This time, static output K is same with equation (2).

Motor made from Ferrite magnet, generally, have output constant as 6~11[kN/m<sup>2</sup>]. Early size of drive motor L<sub>r</sub> can be known, when diameter of rotor is decided.

$$K = \frac{\pi^2 k_{w1}}{4\sqrt{2}} BA \tag{2}$$

Here, k<sub>w1</sub>: carter's coefficient, A: effective value linear

circuit density of around air gap, B: magnetic flux density. For concerning effect of slot having an opening, carter's coefficient has to apply.

### 3.3 Initial Model Design of Drive Motor For Electric Drive Tractor

We incorporated the partition core to the initial model of motor of AEV in order to achieve high efficiency and power density. Also, we can reduce the copper loss by using the concentrated winding to create a shortening effect of the ending part of the coil, and we also applied the flat wire to improve the space factor. The specifications for the initial model are provided on Table2. Fig. 1 shows the initial model that has been created with the correct specifications.

**Table 2.** Initial Model Specifications

Pole number	Pole	8
Slot number	Slot	12
Stator diameter	mm	220
Rotor diameter	mm	128.4
Lamination stack	mm	60
Airgap	mm	0.8
Magnet:Br	T	1.25
S/T steel		S18_0.35T

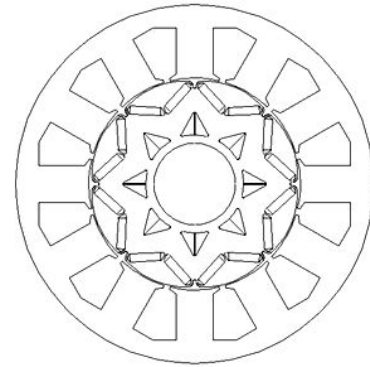


**Fig. 1.** Initial model

### 3.4 Cogging Torque [5]

The variation of the magnetic energy stored in the motor as the PM rotates causes the cogging torque. The cogging torque can be approximated as follows :

$$T_c(\theta) = -\frac{\partial E_g(\theta)}{\partial \theta} \tag{3}$$

where  $\theta$  is the relative position of the PM with respect to the iron core, and  $E_g(\theta)$  is the stored magnetic energy in the air gap of the motor.

In order to calculate the energy stored in the air gap, the field and armature functions are defined. The magnetization function  $B_i(\theta)$ , which represents the distribution of the residual magnetic flux density of the PM, is defined as the magnetic flux density at the air gap when the armature core does not have any slot. The field function  $F(\theta)$  is defined as the magnetic energy density at the air gap, as shown in Fig. 2, and can be expressed using Fourier expansion as follows [6]:

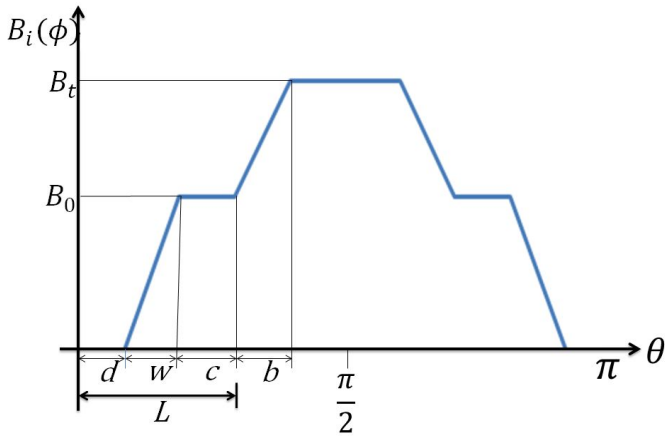


Fig. 2 . Equivalent magnetization distribution of V-type IPM motor

$$F(\theta) = \frac{B_i^2(\theta)}{2\mu_0} = X_0 + \sum_{k=1}^{\infty} X_k \sin\left(kP\theta + \frac{\pi}{2}\right) \quad (4)$$

$$B_0(\theta) = \frac{4B_0}{(wn^2\pi)} [\sin(dn) - \sin(n(d+w))] \sin(n\theta) \quad (5)$$

$$\{B_t - B_0\}(\theta) = \frac{4(B_t - B_0)}{(bn^2\pi)} [\sin(Ln) - \sin(n(L+b))] \sin(n\theta) \quad (6)$$

$$X_k = \frac{B_0^2}{k\pi\mu_0} (-\sin kd) + \frac{(B_t - B_0)^2}{k\pi\mu_0} (-\sin kL) \quad (7)$$

where P is the number of poles of the PM.

The armature function X and cogging torque equation can be written as follows using Fourier expansion [7]:

$$A(\theta) = Y_0 + \sum_{k=1}^{\infty} Y_k \sin\left(kS\theta + \frac{\pi}{2}\right) \quad (9)$$

$$Y_0 = \frac{A_m}{\pi} \cdot (\pi - q) \quad (10)$$

$$Y_k = -\frac{2A_m}{k\pi} \cdot (\sin kq) \quad (11)$$

$$T_c(\theta) = \pi \sum_{n=1}^{\infty} (nGX_{nG}Y_{nG}) \sin(nG\theta + X_{nG} - y_{nG}) \quad (12)$$

where S is the number of slots of the armature core, X is the air-gap volume per unit angle, q is half of the slot width and G is the least common multiplier of P and S.

This paper deals with a reduction of cogging torque through variation of residual magnetic flux density at the air gap. Therefore, modification of the rotor surface shape and V-type magnet angle is considered to reduce the harmonic components caused by the non-ideal spatial distortion of the magnetic flux density at the air gap.

### 4. Shape Design of Rotor

#### 4.1 Structures design classified by model

Fig.3 and 4 shows the rotor shape design of the initial model and the suggested model. The magnetic flux density of the suggested model is greater than that of the initial model. It also corrected its air hole position to be close to the sine wave of BEMF and added Ba to correct the flow of equipotential line. Furthermore, it made the degree of magnet as a parameter to choose the degree that minimizes the cogging torque. The initial model, magnetic flux density of the proposed model, and equipotential line are seen in Fig.5 and 6. The proposed model that applied it is shown in Fig.7.

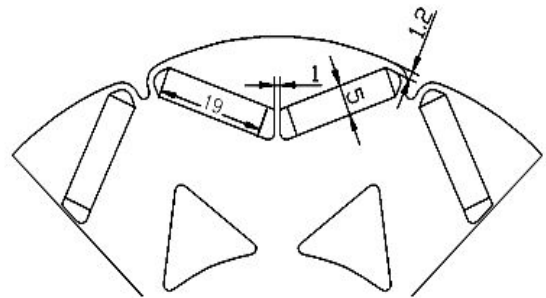


Fig. 3. Design parameters of rotor of initial model

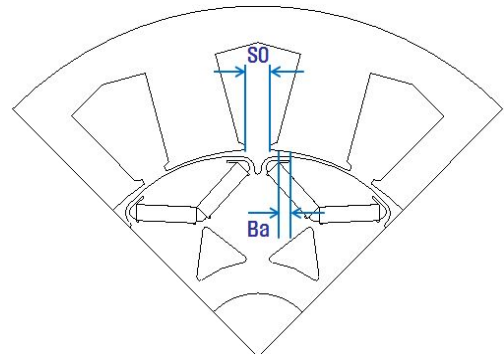


Fig. 4. Design parameters of rotor of proposed model

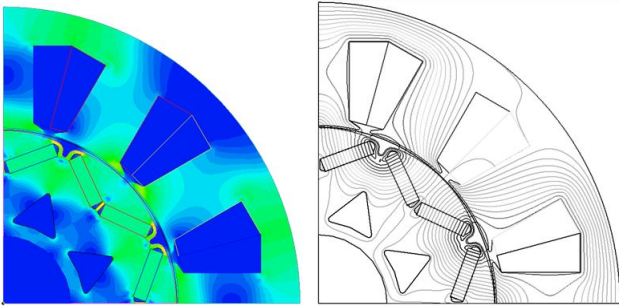


Fig. 5. Magnetic flux density and equipotential line of Initial model

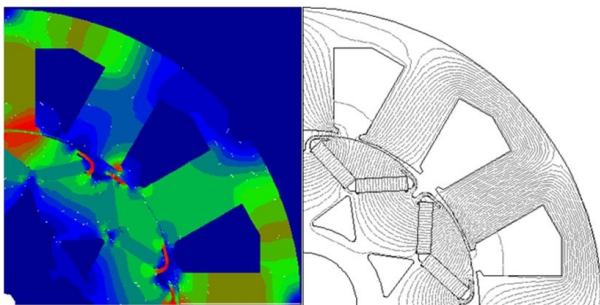


Fig. 6. Magnetic flux density and equipotential line of proposed model

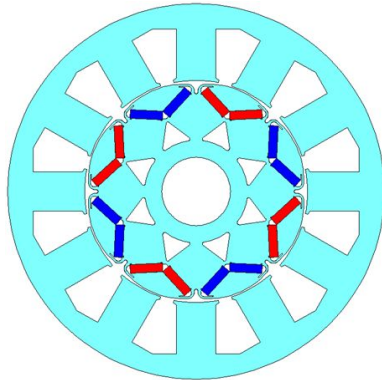


Fig. 7. Propose model

## 5. Comparing with Experiments and Consideration

### 5.1 Back Electromotive Force

Fig.8 is comparison of analyzed BEMF wave. confirm that BEMF for proposed model is bigger than that of initial model. Fig.9 and 10 illustrate waveform of BEMF of the initial model and suggested model. With the waveform of suggested model, we can see that it is improved in the form of a sine wave. When compare analysis value and measurement value, the size of BEMF is similar. Also, Fig. 11 and 12, which analysis the harmonic wave of BEMF

waveform of the initial and suggested model, show that the effect of the harmonic wave is improved as the 5 harmonic wave is improved 2.9% in the initial model and 1.8% in the suggested model.

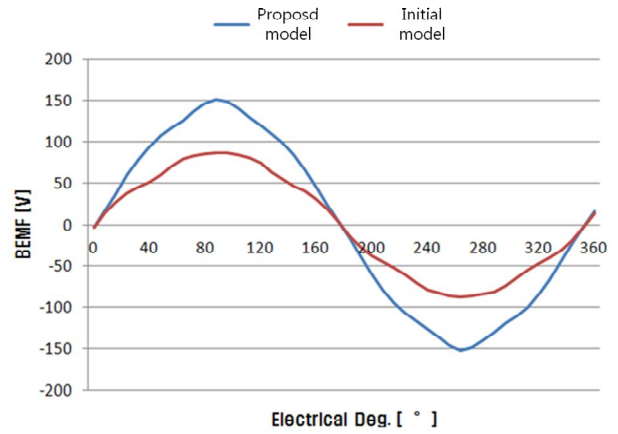


Fig. 8. BEMF compare at 3000[rpm]

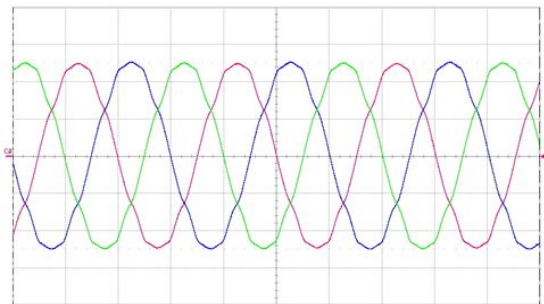


Fig. 9. BEMF of initial model at 1,000[rpm, 10V/div.]

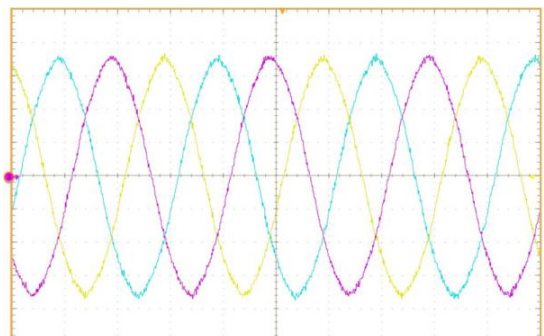


Fig. 10. BEMF compare at 3000[rpm] BEMF of proposed model at 1,000[rpm, 10V/div.]

### 5.2 Cogging Torque

Fig.13 is comparison of cogging torque analysis for initial model and proposed model. As cogging torque of initial model is 1.97[Nm] and that of proposed model is 0.22[Nm], cogging torque of proposed model shows around 88.8% reduction in comparison to initial model. To justify the interpretation value, Fig.14 and 15 shows the actual

estimate value of cogging torque. Fig.16 shows the equipment components for measuring the cogging torque. Looking at cogging torque estimate value, one can see that the basic model value of 1.6[Nm] closely corresponds to the proposed model value of 0.47[Nm]. Cogging torque of such proposed model is 1.5% of constant torque, where I can know it is quite good level.

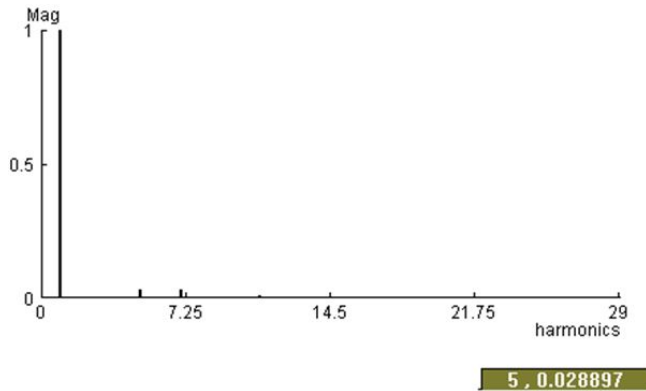


Fig. 11. Harmonic wave of BEMF of initial model

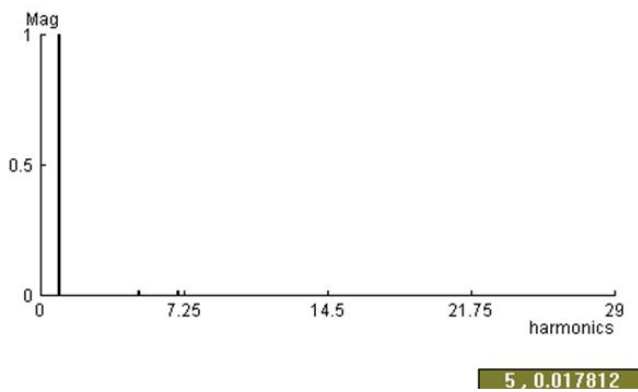


Fig. 12. Harmonic wave of BEMF of proposed model

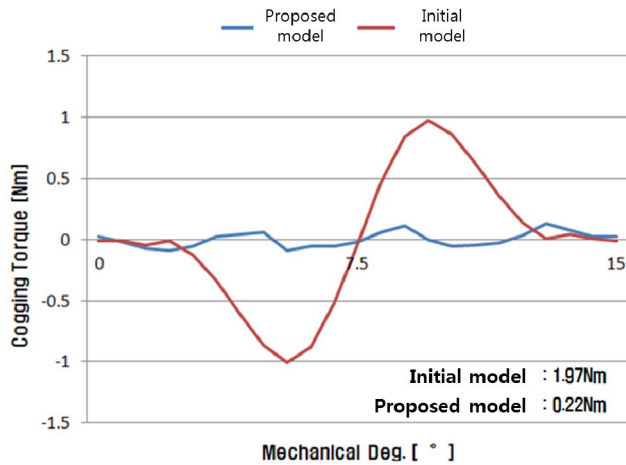


Fig. 13. Cogging Torque compare

### 5.3 N-T-I Characteristics

Fig 17 shows N-T-I special experimental equipment components, Fig. 18 shows the experimental result of the N-T-I characteristics. When it comes to the N-T-I characteristics at the rating output is 10[kW], velocity is 3000[rpm], torque is 32[Nm], phase current is 45[Arms], motor efficiency is 95%. And all of these values satisfy the design specification.

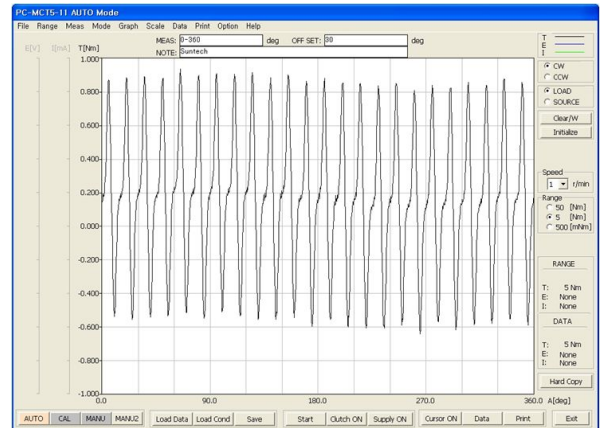


Fig. 14. Cogging Torque of initial model

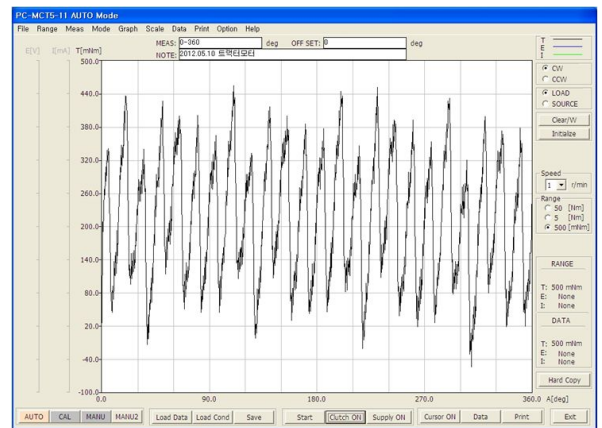


Fig. 15. Cogging Torque of proposed model

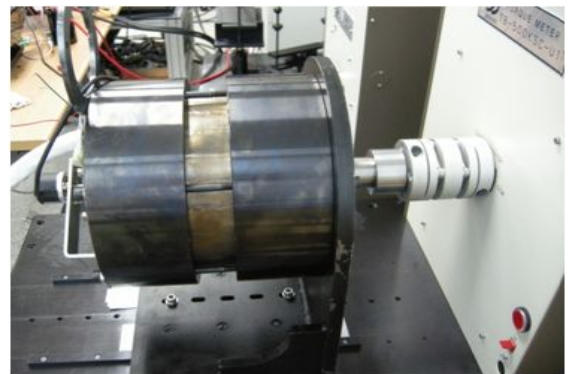


Fig. 16. Equipment components for measuring the cogging torque



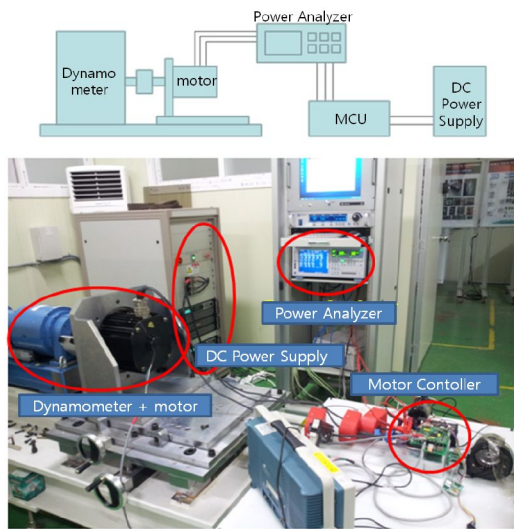


Fig. 17. Equipment components of N-T-I characteristics

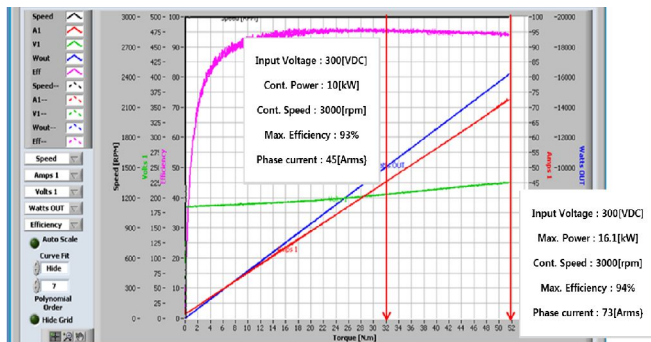


Fig. 18. N-T-I graph

### 6. Conclusion

This paper presents the optimal rotor shape design of IPMSM for reduction of cogging torque. The design parameters are derived by analytical method and rotor surface shape and V-type magnet angle are optimized by using FEM.

The FE analysis and experimental results have proved that the proposed rotor shape design method can reduce the cogging torque and improve efficiency. In addition, since the cogging torque is strongly is related to vibration and noise, the optimized model is very effective at the vibration suppression of the AEV.

### Acknowledgements

This work was supported by the New & Renewable Energy of the Korea Institute of Energy Technology Evaluation and Planning (KETEP) grant funded by the Korea government Ministry of Knowledge Economy. (No. 20113030060010)

### References

- [1] A. Oida et al., "Study on performance of a model electric off-road vehicle," *Agricultural Engineering International: The CIGR Journal of Scientific Research and Development*, vol. IV, Oct. 2002, Manuscript PM 01 008.
- [2] C. C. Chan, "An overview of electric vehicle technology," *Proc. IEEE*, vol. 81, no. 9, Sep. 1993.
- [3] K. Y. Hwang, "A Study on Optimal Pole Design of Spoke-Type IPMSM With Concentrated Winding for Reducing the Torque Ripple by Experiment Design Method", *IEEE Transaction on magnetic*, vol. 45, NO. 19, pp4712-4715, OCTOBER 2009
- [4] C. S. Koh, and J.-S. Seol, "New cogging-torque reduction method for brushless permanent-magnet motors", *IEEE Trans. On magnetic*, vol. 39, no. 6, pp. 3503-3506, Nov. 2003.
- [5] G.H. Kang, Y. D Son, G.T. Kim, and J. Hur "A novel cogging torque reduction method for interior-type permanent-magnet motor", *IEEE Trans. on Industry Applications*, vol. 45, No. 1, pp. 161-167, Jan./Feb. 2009.
- [6] J. Hur, J.-W. Reu, B.-W. kim and G.-H.Kang, "Vibration reduction of IPM-type BLDC motor using negative third harmonic elimination method of air-gap flux density", *IEEE Trans. on Industry Applications*, vol. 47, No. 3, pp. 1300-1309, May/June 2011.



**Ju-Hee Cho** received his B.S. degree in Electronics Engineering and M.S. degree in Department of Electronics, Control and Instrumentation Engineering from Hanyang University in 2001 and 2003, respectively. 2004, he was an engineer in the Central Research Institute, Hyundai Rotem. From 2005 to 2009, he worked for Komotek Co., as a Senior-Researcher. He is currently a Senior-Researcher at the Korea Electronics Technology Institute. His research interests are analysis and design of permanent magnet synchronous motor.



**Yong-Un Park** received his B.S. degree in Electrical Control Engineering from Suncheon National University, Korea. He is currently a M.S. degree student in Electrical Engineering at Suncheon National University. His research interests are the design and analysis of BLDC motor.



**Dae-kyong Kim** received his M.S. degree in Electrical Engineering and his Ph.D. degree in the Department of Electronic, Electrical, Control and Instrumentation Engineering from Hanyang University, Korea in 2001 and 2007, respectively. From 2001 to 2005, he was a Senior Engineer in the Home Appliances R&D Center where he was engaged in research

and development of sensorless motor drive systems for refrigerator and air-conditioner at the Samsung Electronics, Korea. From 2005 to 2011, he was a Center Director of Digital Convergence Center at the Korea Electronics Technology Institute (KETI). Since 2011, he has been with the Department of Electrical Control Engineering, Sunchon National University, Korea as an assistant professor. His current research is in analysis, design, and drives of electrical machines for energy saving and high-performance. He received several Best Paper Awards from the Korea Institute of Electrical Engineers (KIEE), ICEMS2007 and IEEE INTELEC2009. He received a R&D award from Samsung Electronics, a staff award from Korea Electronics Technology Institute (KETI) and a mayor award from Gwangju-city, Korea. He served as Co-chairs and secretary for IEEE INTELEC2009, ICEMS2010, IEEE VPPC2012, and CEFC2012, and other domestic and international conferences.